MNRAS 000, 1–6 (2015) Preprint 14 July 2022 Compiled using MNRAS LATEX style file v3.0

A survey of spectro-temporal properties from FRB20121102A

Mohammed A. Chamma[1]★ and Martin Houde,[1]†
[1]Department of Physics and Astronomy, The University of Western Ontario, 1151 Richmond Street, London, Ontario N6A 3K7, Canada

14 July 2022

ABSTRACT

We survey the spectro-temporal properties of fast radio bursts from FRB20121102A across a wide range of frequencies in an effort to study if all the bursts from a single source obey the same relationships or if multiple classes emerge. We investigate 138 bursts from FRB20121102A spanning frequencies 1-7.5GHz, durations of <1ms-10ms, and low and high energy bursts. We find from our sample of bursts from FRB20121102A a strong agreement with the inverse relationship between sub-burst slope and duration and with other predictions made by the relativistic dynamical model introduced by Rajabi et al. 2020 and for which Chamma et al. 2021 found agreement with across three different sources. For this sample of bursts, we find that the sub-burst slope as well as the drift rate are quadratic with frequency, that both these quantities are inversely proportional to the duration as well as finding that the duration decreases with increasing frequency. No significant group of bursts in this sample deviated from these relationships. This study demonstrates the consistent existence of a relationship between the spectro-temporal properties of bursts from an FRB source regardless of the frequency, energy, or duration of the burst observed.

Key words: fast-radio-burst – dynamical – relativistic

1 INTRODUCTION

Fast radio bursts (FRBs) are short and intense pulses of radiation whose emission mechanism eludes understanding despite a multitude of theoretical models and many recent observational efforts. Observationally, the originating environments, energy distributions, polarization properties, and activity cycles of FRB sources have been investigated with each new study often adding a new unexpected characteristic (Petroff et al. 2022). Theoretical explanations for FRBs center around extreme environments such as magnetars where large numbers of particles in a plasma state emit coherently (Lyubarsky 2021). This flurry of activity around FRBs has revealed significant challenges in understanding this phenomena and in constraining the possible explanations.

Many of the observational characteristics of FRBs vary dramatically from source to source, making it unclear which features are arising due to the emission mechanism, the environment, or propagation effects. The spectral luminosities of FRB sources spans several orders of magnitude and the durations of bursts can range from the tens of nanoseconds to the tens of milliseconds (Nimmo et al. 2021). The polarization properties of FRBs vary as well; for example in FRB20121102A bursts have a constant polarization across their duration (Michilli et al. 2018), whereas in FRB20180301A the polarization angle of some bursts show diverse behaviours (Luo et al. 2020). In FRB20190520B, the range of rotation measures (RMs) observed are the largest observed for any type of astrophysical source studied, including other FRB sources (Anna-Thomas et al. 2022). These characteristics of FRB sources complicate our understanding and are likely due to an overlap of multiple different phenomena.

One avenue for understanding the emission mechanism of FRBs is to study the spectro-temporal properties of bursts, which has revealed several relationships that are common from burst to burst and even from source to source. Among these quantities, which include the bandwidth, duration, and central frequency, are the drift rate and the similar but distinct sub-burst slope or intra-burst drift[1]. The drift rate refers to the change in frequency of multiple resolved sub-bursts within a single waterfall, and the tendency for later sub-bursts to arrive at lower frequencies is called the "sad trombone" effect. The sub-burst slope on the other hand refers to the change in frequency with time within a single sub-burst or pulse. Hessels et al. (2019) studied bursts from FRB20121102A and the relationship between their frequency and the drift rate of multiple resolved sub-bursts, finding that the drift rate increased with frequency. This relationship appeared to be linear (Josephy et al. 2019). In the relativistic dynamical model proposed by Rajabi et al. (2020), an inverse relationship was predicted between a sub-burst's slope and its duration and agreed with measurements made for a sample of bursts from FRB20121102A. This relationship was further explored in Chamma et al. (2021) where bursts analysed from three repeater sources (FRB20180916B and FRB20180814 in addition to FRB20121102A) also had sub-burst slopes that varied inversely with duration, indicating that the same relationship could describe the features of bursts from different sources. The model in Rajabi et al. (2020) also predicted a quadratic relationship between the sub-burst slope and the frequency, and some

★ E-mail: mchamma@uwo.ca
† E-mail: mhoude2@uwo.ca

[1] The 'sub-burst slope' terminology was used in Chamma et al. (2021) while 'intra-burst drift' was used in Jahns et al. (2022). Both terms describe the same measurement and we will use 'sub-burst slope' hereafter.

evidence of this can be seen in various datasets as plotted in Fig. 8 of Wang et al. (2022). Jahns et al. (2022) studied over 800 bursts from FRB20121102A in the 1.1-1.7 GHz band and also found the sub-burst slope to be inversely proportional to duration. In addition they compared the sub-burst slope to a dozen drift rates and found that the drift rates were larger but seemed to extend the same trend with the duration as the sub-burst slopes do (Jahns et al. 2022). This behaviour for drift rates and sub-burst slopes obeying similar or identical relationships is possible within the relativistic dynamical model when groups of sub-bursts are emitted at roughly the same time (Sec. 3.1 of Chamma et al. 2021; Rajabi et al. 2020). Given these recent discoveries it is fruitful to study the spectro-temporal features of bursts in order to better characterize these relationships, to find their limitations, and to find possible commonalities between sources that will contribute to our understanding of the FRB emission mechanism.

In this work we investigate if the same spectro-temporal relationships, such as the relationship between the sub-burst slope and the duration, are followed for a large and diverse sample of bursts from a single source as this will indicate if bursts from a single source can be differentiated based on the spectro-temporal relationships they obey as well as the robustness of these relationships. To this end we collect bursts from multiple observational studies of the repeating source FRB20121102A, one of the best observed repeaters with bursts that cover a wide range of frequencies and durations, and measure their spectro-temporal properties. Our measurements include the central frequency, the sub-burst slope, the sad-trombone drift rate (when applicable), and the duration of every burst, and we investigate the relationships between these quantities, as well if a single relationship is sufficient to describe the data or if deviations exist.

The following sections will describe the bursts sampled for this study, the methodology for measuring the spectro-temporal properties of bursts, and the relationships observed between these quantities.

2 SAMPLED BURSTS FROM FRB20121102A

We list here the observations used and the properties of the bursts sampled for our study.

Michilli et al. (2018) observed 16 bursts from FRB20121102A using the Arecibo observatory in a band that spanned 4.1-4.9 GHz. We use all the bursts they observed and seperated the components of three of their bursts (M9, M10, and M13) for a total of 19 single pulses. The durations of these bursts as measured by their FWHM and excluding the bursts whose components we have separated range from 0.03 ms to 1.36 ms (Michilli et al. 2018).

Gajjar et al. (2018) observed 21 bursts from FRB20121102A using the Green Bank Telescope in a band of 4-8 GHz all of which were 100% linearly polarized and no circular polarization. Of these observations we exclude 5 due to their low SNR and split three of their bursts (11A, 12A, and 12B) for a total of 21 single pulses, with durations that range 0.18 to 1.74 ms (Gajjar et al. 2018).

Oostrum et al. (2020) observed 30 bursts from FRB20121102A using the WSRT/Apertif telescope in a band spanning 1250-1450 MHz (and 1220 to 1520 MHz for one burst) with much lower levels of linear polarization than observed at higher frequencies. We use 24 of these bursts with the remaining six excluded due to low SNR, and all bursts from this dataset were single pulses. The durations of these bursts, as measured by a top hat pulse with an equivalent integrated flux density, spans 1.6 to 8.2 ms (Oostrum et al. 2020).

Aggarwal et al. (2021) searched data collected by Gourdji et al. (2019) using the Arecibo telescope in a band spanning 580 MHz centered around 1.4 GHz and, including the 41 bursts found by Gourdji et al. (2019), found a total of 133 bursts in three hours of data. Notably, almost all of these bursts occur above 1300 MHz. Of these bursts we exclude almost half due to a low SNR and separate 6 into single pulses for a total of 63 bursts. The durations of the bursts used span 1.16 ms to 17.16 ms based on the FWHM obtained from the burst autocorrelation (see Section 3).

Li et al. (2021) used the FAST telescope to detect 1652 bursts in about 60 hours of data over 47 days in a band spanning 1000 to 500 MHz. These bursts followed a bimodal energy distribution with peaks around $10^{37.8}$ and $10^{38.6}$ erg as well as a bimodal wait time distribution with peaks at around 3.4 ms and 70 s. Aggarwal (2021) argued that the bimodality in the energy distribution is due to the burst energies being estimated using the center frequency instead of the bandwidth, where, due to the band-limited and Gaussian-like nature of FRBs, the bandwidth should be used instead. Using the bandwidths found by Li et al. (2021), Aggarwal (2021) calculated the burst energies and found that they did not show any bimodality, suggesting that the different energy distributions seen thus far are due to a bias introduced by limited observing bands. Jahns et al. (2022) found only a weak bimodality in the burst energy distribution in their sample of 849 bursts and could not confirm the result of Li et al. (2021). Nonetheless, in order to investigate if these differing properties correspond to different spectro-temporal features we sampled 20 bursts from both peaks (10 each) of the energy distribution reported by Li et al. (2021) by filtering their list of bursts to those with estimated energies between $10^{37.7}$ and $10^{37.8}$ erg for the first peak and $10^{38.6}$ and $10^{38.7}$ erg for the second peak. To select bursts with high enough SNR for a good measurement we additionally filter bursts from the first peak that have a peak flux greater than 10 mJy and greater than 100 mJy from the second peak. We also sampled bursts from the two peaks of the wait-time distribution, filtering for bursts with wait-times between 4 ms to 6 ms and with a peak flux above 40 mJy, and wait-times between 63 s to 100 s above 100 mJy. This yielded 11 and 13 bursts from each peak, respectively, for an additional 24 bursts. We also sampled a single long duration burst found, as the bursts in this dataset are among the longest ever observed. Of this sample, several more were excluded due to an SNR that was still too low to obtain measurements and many of the short waittime bursts were split into multiple components, which finally resulted in a total of 42 single pulses. The bursts used span a frequency range of 1080-1430 MHz and their FWHM durations span 0.56-15.43 ms.

The sample of bursts analysed in this study total 169 and broadly represent all the types of bursts that have been observed from FRB20121102A, spanning frequencies ranging from 1080 MHz to 7.4 GHz and durations from less than 1 ms to about and greater than 10 ms. Figure 1 shows a distribution of the frequencies and durations of the bursts used in our sample.

3 METHODS AND ANALYSIS

This section will describe how the burst waterfalls are loaded and their spectro-temporal properties measured via 2D autocorrelations of the waterfall (Hessels et al. 2019; Chamma et al. 2021), as well as the dispersion measure (DM) ranges used for the measurements, and how measurements are reviewed and validated. We also describe a graphical user interface (GUI) we developed to aid in the measurement of burst properties that is easily extensible and publicly available.

The FRB observations described in Section 2 were obtained from the authors of their respective publications and we pre-process them

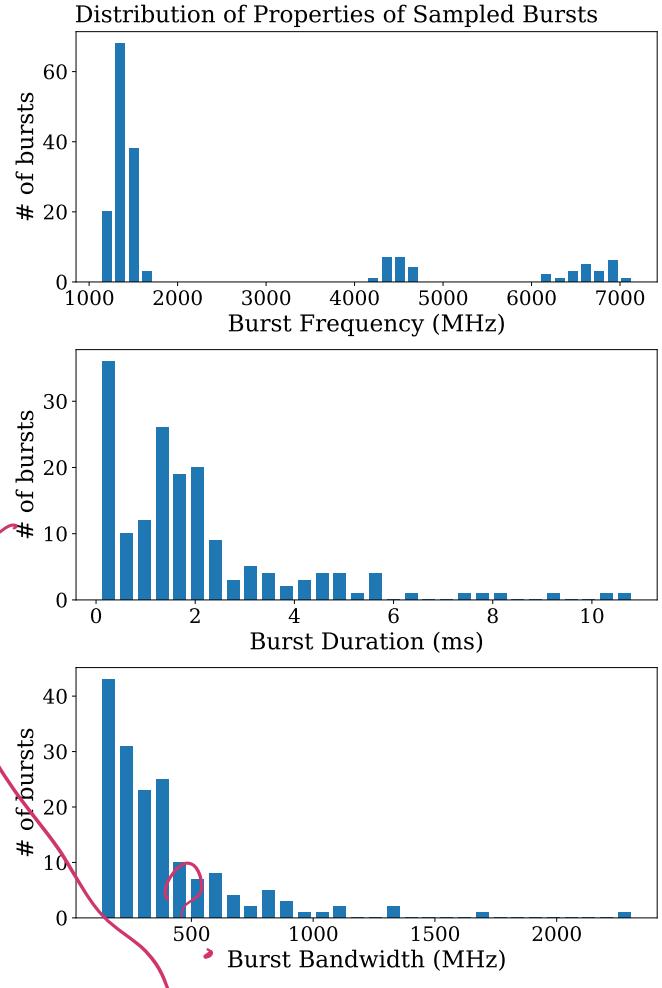

Figure 1. Histograms of the bursts sampled for this study showing the frequency (top) and burst durations (bottom).

in order to increase signal-to-noise (S/N), remove radio frequency interference (RFI), and/or crop bursts before performing measurements. FRB waterfall data is available in various formats and the formats of the data used here include `filterbank` and `PSRFITS` files, which were loaded using the PyPulse[2] and Your[3] software packages before being stored as 2D Python `numpy` arrays. The waterfalls of bursts from Michilli et al. (2018) were provided via an ASCII dump, dedispersed, and are at frequency and time resolutions of 1.5625 MHz and 0.01024 ms, respectively, with 512 frequency channels and 512 time samples (ie. with dimensions 512 x 512). Burst waterfalls from Gajjar et al. (2018) were available dedispersed in `PSRFITS` format at a resolution of 183 kHz and 0.01024 ms with 19456 frequency channels and 2048 time samples, which we subsampled in frequency by a factor of 8 to obtain 2432 frequency channels at a resolution of 1.464 MHz. These were then stored in arrays of size 1690 x 2048 to exclude masked channels present at the bottom of the band. Waterfalls from Oostrum et al. (2020) were obtained un-dedispersed in the `PSRFITS` format with resolutions of about 0.195 MHz and 0.04096 ms with size 1024 x 25000 channels, which we dedispersed to each burst's reported DM and downsampled by a factor of 8 to resolutions of 1.5625 MHz and 0.32768 ms. These waterfalls were then centered and cropped to be stored at a size of 128 x 200 channels. In addition, before downsampling we applied both a spectral kurtosis and Savitzky-Golay filter (SK-SG filter; Agarwal et al. 2020; Nita et al. 2016) that is available via the Your package to mask channels with high RFI. The waterfall data from Aggarwal et al. (2021) are provided in long duration filterbank files with a list of candidate timestamps, and the Burstfit[4] package is used to dedisperse the data to each burst's DM and select a 0.1 s long waterfall around the burst. These waterfalls are then saved as arrays of size 64 x 1220 at resolutions of 12.5 MHz and 0.08192 ms, respectively. Data from Li et al. (2021) were obtained via correspondence and consisted of PSRFITS files for each burst. We load these with Your at a size of 4096 x 131072 channels and resolutions of 122 kHz and 0.098304 ms and then filter them with the SK-SG filter. We then dedisperse each waterfwall to the reported burst DM, subsample to 256 frequency channels, center about the time channel with the peak frequency-averaged intensity and crop to an array of size of 256 x 1000 with resolutions of 1.952 MHz and 0.098304 ms. All the bursts in this study are preprocessed in the way described in order to facilitate the measurements of their spectro-temporal features.

Despite the preprocessing of the waterfalls there are still several tasks that are needed on a burst-by-burst basis, that, with a large number of bursts and measurements to manage, can quickly become overwhelming and difficult to review. These tasks include additional noise removal, additional subsampling to increase the S/N, and separating the components of bursts with multiple pulses. While these tasks can be automated to an extent, being able to manage and customize a measurement allows for more accurate results and the inclusion of strange bursts that might not fit in an automation pipeline of limited complexity. To this end we developed an extensible graphical user interface (GUI) called Frbgui that allows a user to input additional masks, change the subsampling of the data, and isolate components of a burst, and used it to prepare bursts and obtain measurements of the spectro-temporal features.

The spectro-temporal features of burst each are obtained via a 2D Gaussian fit to the 2D autocorrelation of the burst waterfall. An autocorrelation of the waterfall helps increase the S/N for measurement and limits the effect of spectral structures, noise, and banding in the burst and the Gaussian model of the autocorrelation provides an analytical and robust way of measuring the spectro-temporal features from a small number of parameters. This technique is detailed in Appendix A of Chamma et al. (2021) (for example), and for this study, the Gaussian fit is obtained using the physical coordinates of the autocorrelation. Thus, though the dimensions of the Gaussian model's parameters are unitless, the inputs are normalized by the units of the autocorrelation's axes and we obtain

$$G\left(\frac{x}{1\,\mathrm{ms}}, \frac{y}{1\,\mathrm{MHz}}\right) = C \exp\left\{-\frac{1}{2}\left[(x-x_0)^2\left(\frac{\cos^2\theta}{b^2}+\frac{\sin^2\theta}{a^2}\right)\right.\right.$$
$$+2(x-x_0)(y-y_0)\sin\theta\cos\theta\left(\frac{1}{b^2}-\frac{1}{a^2}\right)$$
$$\left.\left.+(y-y_0)^2\left(\frac{\sin^2\theta}{b^2}+\frac{\cos^2\theta}{a^2}\right)\right]\right\}, \quad (1)$$

where C, x_0, y_0, a, b, and θ are the model parameters corresponding to the amplitude, central x- and y- positions, the standard deviations of the Gaussian, and the orientation of the semi-major axis (a) measured from counterclockwise from the positive y-axis. The fit is found

[2] https://github.com/mtlam/PyPulse
[3] https://github.com/thepetabyteproject/your
[4] https://thepetabyteproject.github.io/burstfit/

using the `scipy.optimize.curve_fit` package and we found that the use of physical coordinates when obtaining this fit improves the accuracy of the sub-burst slope measurements by almost 40% when the burst is nearly vertical. The sub-burst slope and burst duration are obtained via equations A2-A3 of Chamma et al. (2021), with the modification that the unit conversion becomes unity due to the choice of coordinates when obtaining the Gaussian fit, so that

$$\frac{d\nu_{\rm obs}}{dt_{\rm D}} = -\left(1\,\frac{\rm MHz}{\rm ms}\right)\cot\theta, \tag{2}$$

$$t_{\rm w} = (1\,{\rm ms})\,\frac{ab}{\sqrt{b^2\sin^2\theta + a^2\cos^2\theta}}, \tag{3}$$

where $d\nu_{\rm obs}/dt_{\rm D}$ and $t_{\rm w}$ are the sub-burst slope and sub-burst duration[5], respectively, and $\nu_{\rm obs}$ and $t_{\rm D}$ are the frequency and delay time (or arrival time) of the burst, written in the formalism of Rajabi et al. (2020). We also compute the total bandwidth $B_{\rm tot}$ according to

$$B_{\rm tot} = (1\,{\rm MHz})\,2\sqrt{2\ln 2}a\cos\theta, \tag{4}$$

which is the semi-major axis of the Gaussian ellipsoid scaled to its full-width-half-max value and projected on to the frequency axis. Figure 2 shows an example measurement of the spectro-temporal properties of burst B006 from Aggarwal et al. (2021). Numerically, equation (2) is equivalent to finding the line that connects the peaks of each row of the autocorrelation and finding the corresponding slope, while equation (3) is equivalent (up to a factor of $2\sqrt{\ln 2}$) to finding the FWHM of the 1D autocorrelation at a frequency lag of zero. For bursts with multiple components in a single waterfall, equations (2) - (4) are still valid and we perform the same analysis to obtain the drift rate. The drift rates we obtain are treated distinctly from the sub-burst slopes as these potentially arise from different phenomena.

Because the choice of DM affects the value of the sub-burst slope and, to a lesser extent, the sub-burst duration, each burst is measured over a range of trial DMs. The DM varies from burst to burst and for a single burst, especially unresolved pulses, the DM might be ambiguous if it is unclear whether to maximize the S/N of the burst or its structure (Gajjar et al. 2018; Chamma et al. 2021, Sec 2.1). We therefore measure each burst over a grid of DMs spanning 555 to 575 pc/cm^3 in steps of 0.5 pc/cm^3, chosen to account for the historical range of DMs observed from FRB20121102A. Each burst is incoherently dedispersed from its reported DM to the trial DM and measured via autocorrelation, resulting in 42 sets of measurements per burst including the reported burst DM. The total set of measurements obtained over the DM grid are then filtered to exclude sub-burst slopes that are positive or with fitting errors larger than 40%. We exclude all positive sub-burst slopes under the assumption that they are unphysical and due to over dedispersion (Chamma et al. 2021). The remaining measurements are then grouped by DM and a fit is found between the sub-burst slope and duration of the form $A/t_{\rm w}$, which is the relationship predicted for these two properties by Rajabi et al. (2020). Of this set of fits, we compute a reduced-χ^2 to assess the goodness of the fit and tabulate the remaining number of bursts for each DM, ie., the number of bursts that passed the filtering process. For each of the datasets listed in Section 2, the range of DMs is limited to only include those DMs that include all the bursts in the sample, and, within this limited range, the DM with optimal (minimal) reduced-χ^2 is chosen as the representative DM for that sample. The range of values in the remaining measurements in the limited DM range are then used as an estimate of the uncertainties. For example, the bursts from Michilli et al. (2018) are measured over the DM range 555-575 pc/cm^3, and, after filtering invalid measurements, the remaining DMs that include all of the bursts range from 555-560 pc/cm^3. Within this limited DM range, the DM with optimal reduced-χ^2 is found to be 558 pc/cm^3, and the range of measurements over the limited DM range are used as the uncertainties of the measurement at 558 pc/cm^3. Treating the measurements of each burst in this manner helps account for the effect of the DM on the measurement and allows for an estimate of the uncertainties beyond those from the Gaussian model.

The measurements are reviewed visually with the help of the bars and slope indicator shown on the left panel of Figure 2. Plots of all measurements can be found online at XXX.

[5] The duration defined in eq. (3) is the correlation length of the burst, and can be converted to other definitions of burst duration with a simple scaling. If the burst is Gaussian with a standard deviation of $\sigma_{\rm p}$ and FWHM $t_{\rm FWHM} = 2\sqrt{2\ln 2}\sigma_{\rm p}$, then the correlation length $t_{\rm w}$ is related to those durations by $t_{\rm w} = \sqrt{2}\,\sigma_{\rm p}$, and $t_{\rm w} = 1/\sqrt{4\ln 2}\,t_{\rm FWHM} \simeq 0.6\,t_{\rm FWHM}$.

4 RESULTS

We describe the results of the autocorrelation analysis performed on all the bursts in this section. The sub-burst slope (normalized by the observing frequency) vs sub-burst duration is shown in Figure X. Figures X-X show the sub-burst duration vs. frequency, the sub-burst slope vs. frequency, and the bandwidth vs frequency. In addition, we show the drift rate vs duration and drift rate vs. frequency in Figure X.

5 DISCUSSION

what does it mean that we didnt see deviations from the relationship

what effect does burst definition have on the A parameter found

what physical parameters can be inferred from the results what does the relativistic model imply for magnetar-centered models

continuing analyses like these will at the very least increase the statistics and can more sharply constrain the physical parameters inferred from our model, and also, can connect the environments of different sources to each other

lets talk about jahns et al

6 CONCLUSIONS

frb20121102a fairly strictly follows the predictions made by the model described in Rajabi et al. (2020)

We studied the spectro-temporal features of bursts from FRB20121102A with frequencies ranging from 1-7.5 GHz and durations ranging from <1ms-10ms as well as low and high energy bursts from several different observational studies (Gajjar et al, Michilli et al., Oostrum et al., Aggarwal et al., and Li et al.) for a total of 134 bursts. In Li et al., a bimodal energy distribution and a bimodal wait time distribution was found for the bursts. We specifically sampled bursts from the two peaks of both bimodal distributions to see if these would follow different trends. No significant deviations from our model were found for this broad sample of bursts, which suggests that these relationships broadly and robustly describe the bursts from this source. In addition, a study by Jahns et al. 2022 studied over 800 bursts from FRB20121102A over narrow frequency band (1-1.5 GHz) and found exactly the relationship predicted in our earlier work. These relationships therefore provide strong quantitative constraints on any theory of the FRB emission mechanism.